and co-workers.[16] These relatively insoluble materials were isolated via metal reduction of diphenyl ditelluride in liquid ammonia and were characterized by elemental analysis.

Summary and Conclusions

We have presented the first detailed study of the synthesis, structure, and reactivity of a wide variety of sterically hindered tellurolate derivatives based on the bulky $^-TeSi(SiMe_3)_3$ ligand. These materials are thermally stable, hydrocarbon soluble, crystalline compounds that are easy to prepare on large scales and in high yields. They show excellent potential as synthetic reagents for the formation of metal-tellurium bonds. Crystal structures of two of these derivatives show the tellurolate anion to be stable either as a partner in a covalent interaction or as the free anion. Further examples of the synthetic potential of these reagents will be reported in due course.

Acknowledgment. We are grateful to the National Science Foundation (Grant No. CHE-90-19675), the Department of Education (fellowship to P.J.B.), and U. C. Berkeley for financial support. We thank Dr. Victor Christou for help with ^{125}Te NMR spectroscopy.

Supplementary Material Available: Details of the structure determinations of **1** and **3**, including tables of temperature factor expressions, positional parameters, and intramolecular distances and angles (11 pages); listing of observed and calculated structure factors (44 pages). Ordering information is given on any current masthead page.

Organotransition-Metal Metallacarboranes. 25.[1] Redox Chemistry and Electronic Studies of Mono- and Dinuclear Iron(II)/Iron(III) Sandwich Complexes

Martin Stephan,[2a,b] James H. Davis, Jr.,[†,2a] Xiangsheng Meng,[2a] Kevin J. Chase,[2a] Jan Hauss,[2b] Ulrich Zenneck,[‡,2b] Hans Pritzkow,[2b] Walter Siebert,*[,2b] and Russell N. Grimes*[,2a]

Contribution from the Department of Chemistry, University of Virginia, Charlottesville, Virginia 22901, and Anorganisch-Chemisches Institut der Universität, D-6900 Heidelberg, Germany. *Received January 22, 1992*

Abstract: The mononuclear 7-vertex *closo*-ferracarborane clusters $(C_5Me_5)Fe^{II}H(Et_2C_2B_4H_4)$ (**1**) and $(C_5Me_5)Fe^{III}(Et_2C_2B_4H_4)$ (**2**) and the phenylene-linked diiron species $(Et_2C_2B_4H_4)M(C_5Me_4-C_6H_4-C_5Me_4)M'(Et_2C_2B_4H_4)$ (**3**, M = M' = Fe^{II}H; **4**, M = Fe^{II}H, M' = Fe^{III}; and **5**, M = M' = Fe^{III}) were prepared and isolated via column and/or plate chromatography on silica or Al_2O_3. Their chemical interconversion was examined, and the air-stable products were characterized from their ^1H, ^{13}C, and ^{11}B NMR, infrared, UV-visible, mass spectra, and elemental analysis and an X-ray diffraction study of **3**. The crystallographic data established the location of the Fe-H hydrogen atom in each of the two equivalent ferracarborane clusters; this hydrogen is coordinated both to iron and to the neighboring boron atoms in the carborane ligand and can be described as capping an Fe-B-B triangular face. The paramagnetic species **2**, **4**, and **5** were investigated via ESR spectroscopy in toluene and THF between 4.5 and 298 K. Magnetic susceptibility measurements conducted on **4** and **5** showed one and two unpaired electrons, respectively, with strong spin-orbit couplings. The ^1H and ^{13}C NMR spectra of paramagnetic **2** were assigned by recording a series of spectra during quantitative stepwise reduction of the complex in THF-d_8, via a potassium mirror in a sealed NMR tube, to form diamagnetic $\mathbf{2}^-$. The latter anion was characterized from its multinuclear NMR spectra. Cyclic voltammetry was conducted on compounds **1-5**. Although **2** exhibits reversible reduction, oxidation and/or reduction of **1**, **3**, or **4** leads to hydrogen abstraction and the formation of Fe(III) species, detectable from their reversible signals and ESR spectra. Crystal data for **3**: M = 689.0; monoclinic, space group $P2_1/c$; Z = 2; a = 8.698 (2), b = 14.949 (4), c = 14.931 (4) Å; β = 106.54 (2)°; V = 1861 Å^3; R = 0.045 for 4135 reflections having $I > 2\sigma(I)$.

Introduction

The *nido*-$RR'C_2B_4H_4^{2-}$ ligands (R, R' = alkyl) have a remarkable and well-documented ability to stabilize organometallic complexes of both transition metals and main-group elements.[3] This property is particularly evident in mixed-ligand sandwiches in which the C_2B_3 open face of the carborane is η^5-coordinated to a transition metal that is also bound to a hydrocarbon ligand. For example, although π-arene complexes of Fe(III) and Ru(III) are unstable and almost unknown, neutral, diamagnetic sandwiches of the type (arene)$M^{II}(Et_2C_2B_4H_4)$ (M = Fe, Ru) are readily oxidized electrochemically to generate stable (arene)M^{III}-$(Et_2C_2B_4H_4)^+$ cations.[1e,4] Clearly, the properties of these small *nido*-carborane ligands open many opportunities for studying organometallic groups that are otherwise inaccessible. We have exploited this stabilizing power extensively in synthesis and have described the isolation and characterization of novel complex types including linked triple- and tetradecker sandwich oligomers,[5,6] air-stable bimetallic fulvalene complexes,[5] indenylferracarboranes

[†] Present address: Department of Chemistry, Brandeis University, Waltham, MA 02254.

[‡] Present address: Friedrich-Alexander Universität Erlangen—Nürnberg, Erlangen, Germany.

(1) (a) Part 24: Piepgrass, K. W.; Stockman, K. E.; Sabat, M.; Grimes, R. N. *Organometallics*, in press. (b) Part 23: Piepgrass, K. W.; Grimes, R. N. *Organometallics*, in press. (c) Part 22: Chase, K. J.; Grimes, R. N. *Inorg. Chem.* **1991**, *30*, 3957. (d) Part 21: Chase, K. J.; Bryan, R. F.; Woode, M. K.; Grimes, R. N. *Organometallics* **1991**, *10*, 2631. The present paper continues our joint research effort which has been reported in earlier publications; see: (e) Fessenbecker, A.; Stephan, M.; Grimes, R. N.; Pritzkow, H.; Zenneck, U.; Siebert, W. *J. Am. Chem. Soc.* **1991**, *113*, 3061 and references therein.

(2) (a) University of Virginia. (b) University of Heidelberg.

(3) Recent reviews: (a) Grimes, R. N. *Pure Appl. Chem.* **1991**, *63*, 369 (transition-metal complexes). (b) Grimes, R. N. In *Electron-Deficient Boron and Carbon Clusters*; Olah, G. A., Wade, K., Williams, R. E., Eds.; John Wiley and Sons: New York, 1991 (transition-metal complexes). (c) Hosmane, N. S.; Maguire, J. A. In *Advances in Boron and the Boranes* [*Mol. Struct. Energ. Vol. 5*]; Liebman, J. F., Greenberg, A., Williams, R. E., Eds.; VCH: New York, 1988; Chapter 14. (main-group-element complexes).

(4) (a) Merkert, J. M.; Geiger, W. E., Jr.; Davis, J. H., Jr.; Attwood, M. D.; Grimes, R. N. *Organometallics* **1989**, *8*, 1580. (b) Merkert, J. M.; Geiger, W. E., Jr.; Attwood, M. D.; Grimes, R. N. *Organometallics* **1991**, *10*, 3545.

(5) Davis, J. H., Jr.; Sinn, E.; Grimes, R. N. *J. Am. Chem. Soc.* **1989**, *111*, 4784.

0002-7863/92/1514-5214$03.00/0

Table I. 115.8-MHz ^{11}B and 300-MHz ^{1}H FT NMR Data

^{11}B NMR Data

compd[a-c]	$\delta(J_{BH}$, Hz)	rel areas
$(C_5Me_5)FeH(Et_2C_2B_4H_4)$ (**1**)	−7.8 (151), −9.0 (153), −19.6 (144)	2:1:1
$(C_5Me_5)Fe(Et_2C_2B_4H_4)$ (**2**)	327, −486, −530	~2:1:1
$K^+(C_5Me_5)Fe(Et_2C_2B_4H_4)^-$ (**2**$^-$)[d]	−1.5, −12.1	3:1
$[(Et_2C_2B_4H_4)FeH(C_5Me_4)]_2C_6H_4$ (**3**)	−7.8,[e] −19.2 (116)	3:1
$(Et_2C_2B_4H_4)FeH(C_5Me_4)-C_6H_4-(C_5Me_4)Fe(Et_2C_2B_4H_4)$ (**4**)	−7.2, −19.0 (116), −327, −486, −530	1:3:2:1:1
$[(Et_2C_2B_4H_4)Fe(C_5Me_4)]_2C_6H_4$ (**5**)	−331, −478, −534	~2:1:1

^{1}H NMR Data

compd	δ[f-h]
1	2.64 (m, ethyl CH_2), 2.29 (m, ethyl CH_2), 1.82 (s, C_5Me_5), 1.16 (t, ethyl CH_3), −11.21 (sb, FeH)
2	18.92 (sb, ethyl CH_2), 13.17 (sb, ethyl CH_2), −1.61 (sb, ethyl CH_3), −16.76 (sb, C_5Me_5)
2$^-$[d]	2.53 (m, ethyl CH_2), 2.16 (m, ethyl CH_2), 1.79 (s, C_5Me_5), 1.11 (t, ethyl CH_3)
3	7.60 (s, C_6H_4), 2.70 (m, CH_2), 2.29 (m, CH_2), 1.90 (s, C_5Me_4), 1.88 (s, C_5Me_4), 1.14 (t, ethyl CH_3), −10.99 (sb, FeH)
4	16.11 (sb), 14.31 (sb), 4.78 (s, C_6H_4), 2.10 (m, CH_2), 1.83 (m, CH_2), 1.52 (s, C_5Me_4), 1.41 (s, C_5Me_4), 0.81 (t, ethyl CH_3), −1.44 (sb), −11.87 (sb, FeH), −14.15 (sb), −20.99 (sb)
5	15.68 (sb), 13.44 (sb), −1.89 (sb), −15.05 (sb), −20.65 (sb), −25.06 (sb)

[a] Shifts relative to $BF_3{\cdot}OEt_2$, positive values downfield. For complexes **2** and **2**$^-$, the boron-11 and proton spectra were recorded at 64.2 and 200 MHz, respectively. [b] *n*-Hexane solution. [c] H–B coupling constant in Hz is given in parentheses, when resolved. [d] THF-d_8 solution. [e] Overlapping resonances, *J* not measurable. [f] $CDCl_3$ solution. [g] Shifts relative to $(CH_3)_4Si$. Integrated peak areas in all cases are consistent with the assignments given. Legend: m = multiplet, s = singlet, sb = broad singlet, d = doublet, t = triplet, q = quartet. [h] $B-H_{terminal}$ resonances are broad quartets and mostly obscured by other signals.

exhibiting ring migration,[1e] multidecker sandwiches of organic heterocycles,[1c-e] and others.[3a,b]

In an effort to develop a more detailed picture of the electronic structure and properties of carborane–iron–arene systems, we have examined selected monoiron and diiron species in which the metal centers undergo reversible redox as well as protonation/deprotonation processes. Among other things, we were particularly interested in the extent of electron delocalization and metal–metal communication in the diiron complexes and in the nature of metal–arene bonding in these systems in comparison to "conventional" iron–arene sandwich complexes. Such questions bear on current efforts in our laboratories to synthesize electron-delocalized carborane-stabilized organometallic oligomers and polymers.[3a,5,6] In the present work, the electrochemical behavior of selected ferracarborane clusters has been studied via a combined approach employing cyclic voltammetry, NMR, and ESR spectroscopy, from which it is possible to correlate electrochemical data with the observed chemical interconversions in these species.

Results and Discussion

Synthesis and Properties of $Cp^*Fe^{II}H(Et_2C_2B_4H_4)$ (1) and $Cp^*Fe^{III}(Et_2C_2B_4H_4)$ (2). The reaction of pentamethylcyclopentadienide anion ($C_5Me_5^-$) with anhydrous ferrous chloride and the $Et_2C_2B_4H_5^-$ anion in tetrahydrofuran (THF) with subsequent isolation on silica gel afforded orange, slightly air-sensitive crystals of **1** in high yield (Scheme I). Compound **1** was characterized via ^{11}B and ^{1}H FT NMR, infrared, UV–visible, and mass spectra (Table I and Experimental Section). These data are consistent with a diamagnetic iron(II) species having the structure depicted in Scheme I; the presence of an Fe–H hydrogen atom is indicated by the mass spectrum and the characteristic proton NMR high-field signal at δ −11.2 ppm. Further support for this structure was provided by an X-ray diffraction investigation of the closely related diiron species **3** (vide infra) in which the unique metal-bound hydrogens were located.

On exposure to tetramethylethylenediamine (TMEDA) in THF solution[7] in air (or to HCl/Et_2O in air), **1** was nearly quantitatively

Scheme I[a]

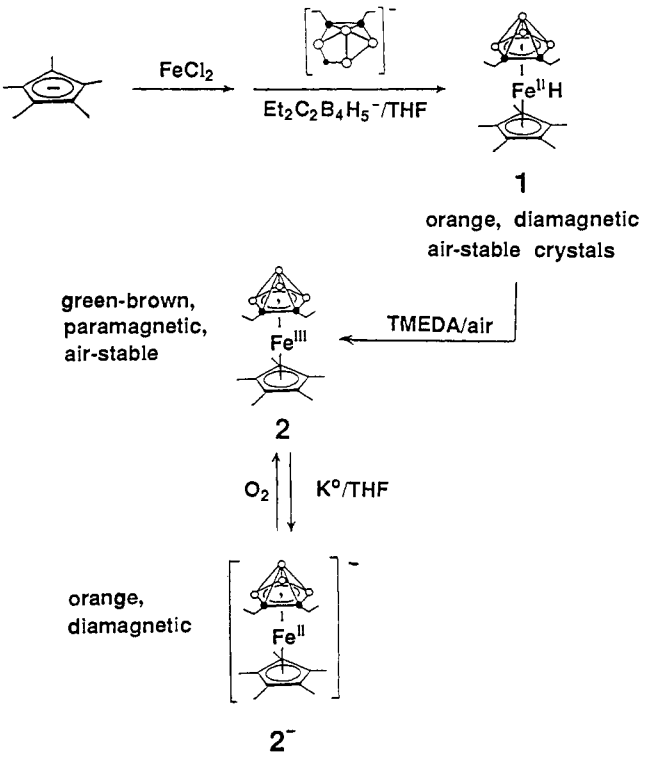

[a] (○) BH, (●) C.

converted to greenish-brown paramagnetic **2** (Scheme I), formulated as an iron(III) complex from its ^{1}H and ^{11}B NMR spectra and its low-temperature ESR spectrum (discussed below). On exposure of **1** to air alone, **2** was very slowly formed as the sole isolable product. The proton and carbon-13 NMR spectra of **2**, a 17-electron complex, were completely assigned via stepwise reduction in THF-d_8 to the 18-electron diamagnetic species **2**$^-$ in a sealed NMR tube which contained a potassium mirror on the tube wall above the liquid surface. Repeated brief contact of the solution with the potassium converted increasing amounts of **2** to the bright orange anion, with recording of the NMR

(6) Meng, X.; Grimes, R. N. Abstracts of Papers, IX FECHEM Conference on Organometallic Chemistry, Heidelberg, Germany, July 1991, Abstract O-21.

(7) Base-promoted "decapitation" (removal of the apex BH group), a commonly observed reaction of $LM(R_2C_2B_4H_4)$ complexes,[3a,b] is not observed with **1**, **2**, the other ferracarboranes described herein, or the analogous η^5-indenylferracarboranes.[1e] In contrast, (η^6-arene)$Fe(R_2C_2B_4H_4)$ complexes[8a,b] *do* undergo this reaction to form the corresponding *nido*-(η^6-arene)Fe-$(R_2C_2B_3H_5)$ species.[8c] In our experience, the only other transition-metal MC_2B_4 clusters that are not decapitated under these conditions are the species $(\eta^8\text{-}C_8H_8)M(Et_2C_2B_4H_4)$ (M = Ti, V).[9]

(8) (a) Maynard, R. B.; Swisher, R. G.; Grimes, R. N. *Organometallics* **1983**, *2*, 500. (b) Swisher, R. G.; Sinn, E.; Grimes, R. N. *Organometallics* **1983**, *2*, 506. (c) Swisher, R. G.; Sinn, E.; Butcher, R. J.; Grimes, R. N. *Organometallics* **1985**, *4*, 882.

(9) Swisher, R. G.; Sinn, E.; Grimes, R. N. *Organometallics* **1984**, *3*, 599.

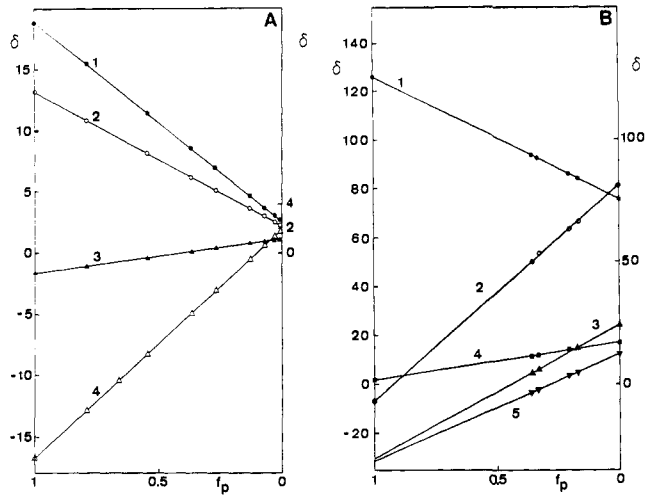

Figure 1. Correlation diagrams for ^1H NMR (A) and ^{13}C NMR (B) signals of $2/2^-$ mixtures (tabulated data are available as supplementary material). Plots in part A: 1 and 2, CH_2; 3, ethyl CH_3; 4, $C_5(CH_3)_5$. Plots in part B: 1, Cp* ring carbons; 2, carborane cage carbons; 3, CH_2; 4, ethyl CH_3; 5, Cp* methyl carbons.

spectrum at each stage so that the signals of **2** were directly correlated with those of the anion as shown in Figure 1 (proton and carbon shifts as a function of $2/2^-$ ratio are listed in supplementary Tables VI and VII). The end point, representing complete conversion to 2^-, was reached when the diamagnetic NMR signals showed no further shift on continued exposure to potassium; thus, the anion is inert to further reduction, an observation which is supported by the electrochemistry presented below. This method has been employed previously in the ^1H NMR characterization of paramagnetic metal–organoborane and metallacarborane complexes.[10] However, the present work marks the first successful use of this approach to obtain a correlated and fully assigned ^{13}C NMR spectrum of a paramagnetic species (in some instances, ^{13}C spectra have been solved by selective decoupling[10a]).

At each stage of the reduction of **2**, we observed an averaged set of ^1H or ^{13}C NMR signals (rather than superimposed spectra of two distinct species), indicating rapid electron exchange between **2** and 2^- which produced a linear relation between δ and f_p, the mole fraction of **2**. Differences in the δ values of the paramagnetic and diamagnetic line positions represent the paramagnetic shift.[11a,b]

The carbon-13 correlation diagram (Figure 1B) shows that the unpaired electron in **2** has a stronger influence on carbon atoms closer to the metal center than on those further away; e.g., the slope of the CH_2 signal is steeper than that of the ethyl CH_3 resonance. The observation of the ^{13}C cage carbon resonance is particularly notable. After pulsing overnight, this broad signal was found at low field (in **2**) near the resonance of the Cp* ring carbons. As the diagram clearly demonstrates, the cage carbon resonance is extremely sensitive to f_p, changing from δ −6.5 in pure **2** to +80.69 in the anion. The latter value is in the normal range for metallacarborane cage carbons; for example, in neutral 18-electron (arene)$Fe(R_2C_2B_4H_4)$ complexes that are isoelectronic with 2^-, it is near +90 ppm.[8a,b] This finding suggests that the electronic environment of the cage carbon region is not greatly different in the anion 2^- than it is in its neutral arene counterparts; the situation in the vicinity of the cage boron atoms, however, is quite different.

The ^{11}B NMR spectrum of 2^- bears comparison with its isoelectronic cobalt analogue $Cp^*Co(Et_2C_2B_4H_4)$, whose signals appear at δ 12.1, 4.3, and 2.6 in a 1:2:1 area ratio.[12] The shift to much higher field in 2^- can be attributed to greater electron density on the boron atoms of the carborane ligand in that species, which is not unexpected since the metal oxidation states in the cobalt and iron complexes are formally +3 and +2, respectively. Moreover, there is a correlation in terms of reactivity: as reported previously,[1e] on treatment with $(Cp^*NiBr)_2$, both 2^- and its indenyl analogue $(\eta^5\text{-}C_9H_7)Fe(Et_2C_2B_4H_4)^-$ undergo polyhedral expansion via insertion of nickel into the B5–B7 bond to form 8-vertex FeC_2B_4Ni clusters, which can be taken as a further indication of a buildup of electron density in that region of the FeC_2B_4 cage.

Table II. Experimental X-ray Diffraction Parameters and Crystal Data for **3**

space group	$P2_1/c$
a, Å	8.698 (2)
b, Å	14.949 (4)
c, Å	14.931 (4)
β, deg	106.54 (2)
V, Å^3	1861
Z	2
μ, cm^{-1} (Mo Kα)	7.5
transmission factors	0.70–0.77
λ, Å	0.7107
D(calcd), g cm^{-3}	1.23
crystal size, mm	0.4 × 0.6 × 0.8
2θ range, deg	3–60
reflectns measd	5643
reflectns obsd	4135
R	0.045
R_w	0.056
largest peak in final diff map, e/Å^3	0.3

Complex **2** furnishes an unusual example of a species for which interpretable NMR and ESR spectra (discussed below) are both obtainable. Signal line widths are largely dependent on the electron spin–lattice relaxation time τ_e, with well-resolved ESR spectra normally obtained when $\tau_e > 10^{-9}$ s and well-resolved NMR spectra observed when $\tau_e < 10^{-11}$ s[11]. In the case of **2**, both a solution $\langle g \rangle$ and an interpretable NMR spectrum are exhibited, allowing both techniques (as well as cyclic voltammetry, vide infra) to be brought to bear on the same species.

Exposure of the 2^- ion to air easily regenerated **2**, as evidenced by its greenish-brown color and its paramagnetic NMR spectrum. Although the analogous cyclopentadienyliron species $CpFe(H)(C_2B_4H_6)$ and $CpFe(C_2B_4H_6)$ were prepared some time ago and shown to undergo similar redox chemistry,[13] the syntheses of **1** and **2** in the present study enabled direct comparison of these monoiron complexes with their diiron counterparts described below.

Synthesis and Properties of Diiron Complexes of the 1,4-Bis(tetramethylcyclopentadienyl)benzenide Dianion. Addition of a THF solution of the $1,4\text{-}(C_5Me_4)_2C_6H_4^{2-}$ dianion[14] to a suspension of anhydrous ferrous chloride in THF, and subsequent reaction with the $Et_2C_2B_4H_5^-$ monoanion, produced a dark solution which on workup gave orange, diamagnetic $[(Et_2C_2B_4H_4)FeH(C_5Me_4)]_2C_6H_4$ (**3**) in 60% isolated yield on a 1.3-g scale (Scheme II).

Air-stable, crystalline **3** is an isoelectronic analogue of the previously reported[5] dicobalt(III) complex $[(Et_2C_2B_4H_4)Co(C_5Me_4)]_2C_6H_4$ and its double-decapitated derivative $[(Et_2C_2B_3H_5)Co(C_5Me_4)]_2C_6H_4$, whose structure was established by X-ray crystallography.[5] The spectroscopic data on **3** support a corresponding geometry, which has been confirmed by an X-ray study as shown in Figure 2. Tables II and III list crystal structure and data collection information and bond distances and angles. All atoms including hydrogens were located in the molecule, which has a crystallographic center of symmetry. The plane of the

(10) (a) Köhler, F. H.; Zenneck, U.; Edwin, J.; Siebert, W. *J. Organometal. Chem.* **1981**, *208*, 137. (b) Zwecker, J.; Kuhlmann, T.; Pritzkow, H.; Siebert, W.; Zenneck, U. *Organometallics* **1988**, *7*, 2316.

(11) (a) Keller, H. J.; Schwarzhans, K. E. *Angew. Chem.* **1970**, *82*, 227. (b) Keller, H. J. *Ber. Bunsenges Phys. Chem.* **1972**, *76*, 1080. (c) Holm, R. H.; Hawkins, C. J., Jr. In *NMR of Paramagnetic Molecules*; Le Mar, G. N., Horrocks, W., Holm, R. H., Eds.; Academic Press: New York, 1973.

(12) Davis, J. H., Jr.; Sinn, E.; Grimes, R. N. *J. Am. Chem. Soc.* **1989**, *111*, 4776.

(13) Sneddon, L. G.; Beer, D. C.; Grimes, R. N. *J. Am. Chem. Soc.* **1973**, *95*, 6623.

(14) Bunel, E. E.; Campos, P.; Ruz, J.; Valle, L.; Chadwick, I.; Santa Ana, M.; Gonzalez, G.; Manriquez, J. M. *Organometallics* **1988**, *7*, 474.

Scheme II[a]

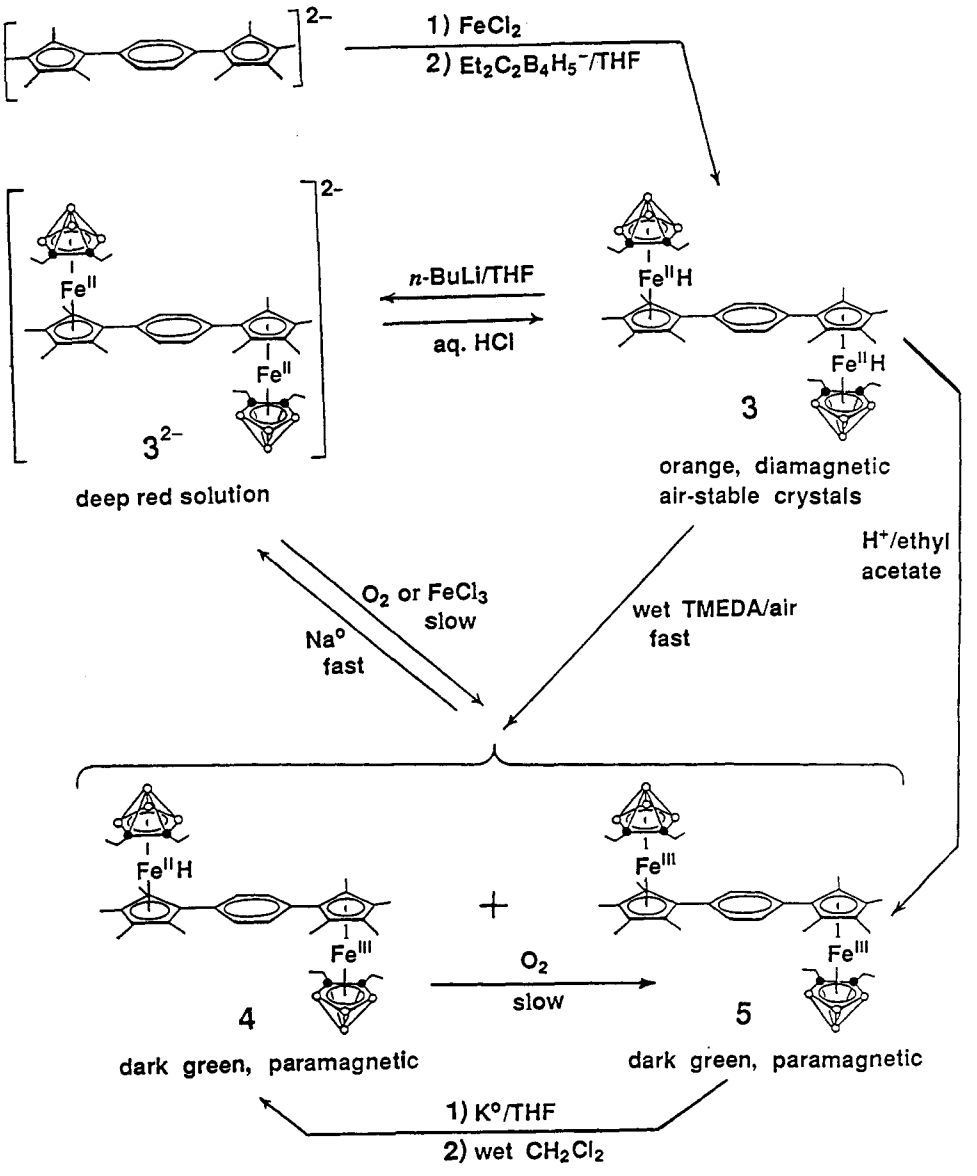

[a] (○) BH, (●) C.

central phenylene ring is tilted by 55° relative to the cyclopentadienyl planes, a finding similar to the corresponding tilts observed in other bis(metallacarboranyl) complexes of the 1,4-$(C_5Me_4)_2C_6H_4^{2-}$ ligand,[5] which range from 47 to 51°. The bond distances and angles in the C_2B_4 cage are close to those previously observed in FeC_2B_4 clusters (see ref 1e and references therein), except for effects that are attributable to the bridging hydrogen atom H1. This atom, a rare example of a crystallographically located hydrogen capping a face of a metallaboron polyhedron (and apparently the first involving iron),[15] is located 1.63 Å from the iron atom and ca. 1.45 Å from B4 and B5, all representing greater than normal single-bond distances but well within bridge-bonding range. H1 is placed 0.9 Å above the Fe–B4–B5 plane. As would be expected, the bond lengths B4–B5, Fe–B4, and Fe–B5 are all significantly longer than normal owing to the presence of H1 over the triangular face; for example, in the indenylferracarborane $(\eta^5\text{-}C_9H_7)Fe(Et_2C_2B_4H_4)$ (which has no

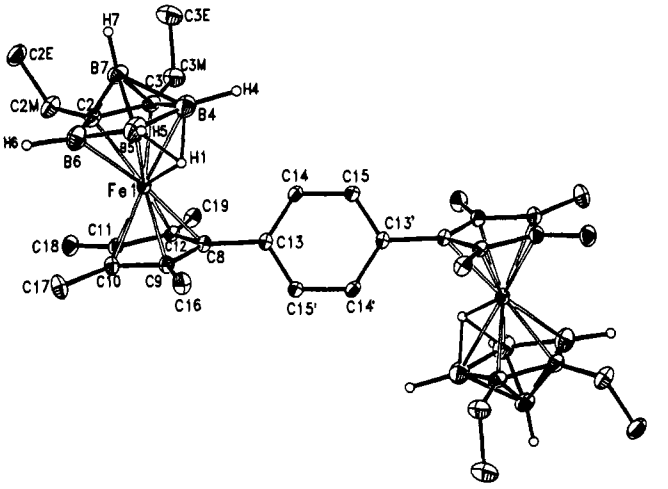

Figure 2. ORTEP diagram of the molecular structure of **3** with 25% probability ellipsoids. Hydrogen atoms other than those bound to boron are omitted for clarity.

(15) Hydrogen atoms capping CoB_2 or Co_2B triangular faces have been located via X-ray diffraction in $Cp_2Co_2B_4H_6$,[16] $Cp_3Co_3B_3H_5$ (bridging hydrogens disordered),[17] and $Cp_4Co_4B_2H_4$.[18] An X-ray structural investigation of the bis(carboranyl)iron complex $(Me_2C_2B_4H_4)_2FeH_2$ failed to locate the Fe–H hydrogens, although their effects on the cage structure are evident.[19]

(16) Pipal, J. R.; Grimes, R. N. *Inorg. Chem.* **1979**, *18*, 252.

(17) Pipal, J. R.; Grimes, R. N. *Inorg. Chem.* **1977**, *16*, 3255.

(18) Feilong, J.; Fehlner, T. P.; Rheingold, A. L. *J. Am. Chem. Soc.* **1987**, *109*, 1860.

(19) Pipal, J. R.; Grimes, R. N. *Inorg. Chem.* **1979**, *18*, 263.

Table III. Bond Distances and Selected Bond Angles for 3

Bond Distances, Å			
Fe1–C2	2.065 (2)	B5–H5	1.247 (29)
Fe1–C3	2.062 (3)	B6–B7	1.800 (5)
Fe1–B4	2.213 (3)	B6–H6	1.227 (27)
Fe1–B5	2.262 (3)	B7–H7	1.038 (30)
Fe1–B6	2.140 (3)	C2M–C2E	1.515 (4)
Fe1–B7	2.778 (3)	C3M–C3E	1.507 (5)
Fe1–C8	2.061 (2)	C8–C9	1.444 (3)
Fe1–C9	2.051 (2)	C8–C12	1.436 (3)
Fe1–C10	2.064 (3)	C8–C13	1.487 (3)
Fe1–C11	2.072 (2)	C9–C10	1.430 (3)
Fe1–C12	2.073 (2)	C9–C16	1.500 (3)
C2–C3	1.470 (4)	C10–C11	1.432 (3)
C2–B6	1.549 (4)	C10–C17	1.500 (4)
C2–B7	1.755 (4)	C11–C12	1.438 (3)
C2–C2M	1.512 (4)	C11–C18	1.492 (3)
C3–B4	1.574 (4)	C12–C19	1.488 (3)
C3–B7	1.783 (4)	C13–C14	1.396 (3)
C3–C3M	1.501 (4)	C13–C15′	1.394 (3)
B4–B5	1.765 (5)	C14–C15	1.383 (3)
B4–B7	1.777 (5)	Fe1–H1	1.629 (30)
B4–H4	1.262 (29)	B4–H1	1.455 (30)
B5–B6	1.697 (5)	B5–H1	1.443 (28)
B5–B7	1.732 (5)		
Bond Angles, deg			
B6–C2–C3	114.0 (2)	C11–C10–C9	107.9 (1)
C2M–C2–C3	122.8 (2)	C17–C10–C9	125.7 (2)
C2M–C2–B6	122.5 (2)	C17–C10–C11	126.3 (2)
B4–C3–C2	113.0 (2)	C12–C11–C10	108.4 (1)
C3M–C3–C2	123.4 (2)	C18–C11–C10	125.9 (2)
C3M–C3–B4	122.4 (2)	C18–C11–C12	125.5 (2)
B5–B4–C3	103.6 (2)	C11–C12–C8	107.7 (1)
B6–B5–B4	103.4 (2)	C19–C12–C8	127.0 (2)
B5–B6–C2	105.8 (2)	C19–C12–C11	125.0 (2)
C2E–C2M–C2	113.5 (2)	C14–C13–C8	122.5 (2)
C3E–C3M–C3	115.0 (3)	C8–C13–C15′	120.0 (2)
C12–C8–C9	107.7 (1)	C14–C13–C15′	117.5 (2)
C13–C8–C9	126.0 (1)	C15–C14–C13	120.9 (2)
C13–C8–C12	125.9 (1)	C14–C15–C13′	121.6 (2)
C10–C9–C8	108.2 (1)	B4–H1–Fe1	91.5 (16)
C16–C9–C8	127.0 (2)	B5–H1–Fe1	94.7 (16)
C16–C9–C10	124.8 (2)	B5–H1–B4	75.0 (14)

bridging hydrogen atoms),[1e] the corresponding distances are about 0.1 Å shorter than in 3.

The cyclopentadienyl ring in 3 is tilted slightly (6.6°) with respect to the C_2B_3 ring plane, in a direction away from H1. It is interesting that in the related dicobalt complex $[(Et_2C_2B_3H_5)Co(C_5Me_4)]_2C_6H_4$, the C_2B_3 ring plane is tilted by 7.2° in the opposite direction, i.e., toward the phenylene group.[5] The difference may be a consequence of the bridging hydrogen H1, but these tilt angles are relatively small and are undoubtedly affected by electronic factors (especially metal orbital contributions) as well as crystal packing forces.

The Fe–H hydrogens in 3 are protonic in character and can be readily removed by *n*-butyllithium in THF, forming the dark red $[(Et_2C_2B_4H_4)Fe^{II}(C_5Me_4)]_2C_6H_4^{2-}$ dianion (3^{2-}); treatment of this species with excess aqueous HCl regenerated neutral 3 quantitatively.

The redox chemistry of 3 and its dianion proved surprisingly complex. Treatment of a solution of 3^{2-} with dioxygen or $FeCl_3$ *slowly* (weeks) generated a mixture of the dark green, paramagnetic complexes $(Et_2C_2B_4H_4)Fe^{II}H(C_5Me_4)-C_6H_4-(C_5Me_4)Fe^{III}(Et_2C_2B_4H_4)$ (4) and $[(Et_2C_2B_4H_4)Fe^{III}(C_5Me_4)]_2C_6H_4$ (5), as shown in Scheme II. The same two species were formed rapidly (in minutes) when a THF solution of neutral 3 was treated with wet TMEDA in air. In both reactions, the major product obtained was the diradical 5. Compounds 4 and 5 were isolated in pure form via chromatography in air on silica, which afforded lustrous black crystals in yields of ca. 8% and 86%, respectively. Alternatively, treatment of 3 with acidified ethyl acetate gave 5 alone, in quantitative yield.

The assigned structures of these paramagnetic species are consistent with their mass spectra, which indicate one and two fewer hydrogens, respectively, for 4 and 5 relative to 3. The NMR data for the bis[iron(III)] compound 5 (Table I) are essentially uninterpretable, but the ^1H spectrum of 4 is entirely consistent with the presence of both diamagnetic and paramagnetic iron centers; thus, the Fe–H proton signal at δ −11.9 is clearly discernible, as are resonances assigned to the phenylene, methylene, ethyl, and pentamethylcyclopentadienyl groups, together with other signals arising from the paramagnetic portion of the molecule. Furthermore, comparison of this spectrum with that of the bis[iron(II)] species 3 shows that in 4, the electronic structures of the C_6H_4 ring and of the $FeH(Et_2C_2B_4H_4)$ cluster unit are only slightly affected by the presence of a paramagnetic Fe(III) center. These data suggest that the unpaired electron in 4 is largely confined to the vicinity of the $Fe^{III}C_2B_4$ cage and is not appreciably delocalized between the two metal centers, a conclusion which is further supported by electrochemical and ESR data presented below. In contrast to this finding, the corresponding biphenyl complex[4a] $(\eta^6\text{-}C_6H_5)_2Fe_2(Et_2C_2B_4H_4)$ undergoes two reversible one-electron oxidations, suggesting extensive Fe–Fe electron delocalization.[4a]

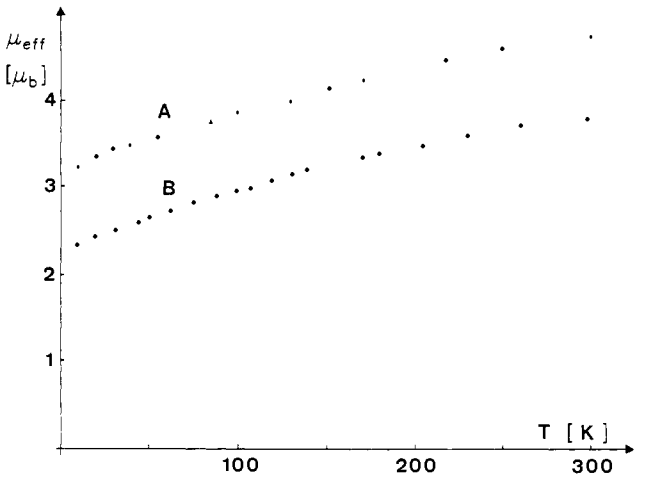

Figure 3. Effective magnetic moment of 4 (B) and 5 (A) as a function of temperature (10–300 K).

Both 4 and 5 were readily reduced to the dianion 3^{2-} on treatment with sodium naphthalenide. Similarly, exposure of 5 to a potassium mirror in THF generated the same red dianion, which on workup in wet CH_2Cl_2 gave a mixture of 3 and 4.

Magnetic Susceptibility Measurements. The data for 4 and 5, measured between 10 and 300 K, are consistent in both cases with simple paramagnetic species. A plot of μ_{eff} vs T, presented in Figure 3, clearly shows the presence of one and two unpaired electrons in 4 and 5, respectively. The data reveal considerable spin–orbit coupling in these complexes, as shown by the deviations from the respective spin-only values of 1.73 and 2.83 μ_B for one and two unpaired electrons; this is consistent with the localization of spin density primarily in metal orbitals.

Electron Spin Resonance Spectroscopy. The 17-electron complex 2 was examined in toluene and THF solutions and glasses between 4.5 and 298 K. At 298 K, a broad signal (~300-G width) with $\langle g \rangle = 2.220$ was measured; at lower temperatures, the signal split, with $g_\parallel = 2.689$ and $g_\perp = 1.979$ at 100 K. Between 100 and 4.5 K, no further changes were observed. The X-band spectrum of 2 at −160 °C is presented in Figure 4. Similar spectra were observed for the diiron species 4: at room temperature, $\langle g \rangle = 2.160$, while at 100 K, $g_\parallel = 2.544$ and $g_\perp = 2.010$. The distinct g-tensor anisotropy in these species is consistent with observations in previously studied iron sandwich complexes.[4,20] Together with the magnetic susceptibility measurements discussed above, as well as the ^1H and ^{11}B NMR spectra, these data demonstrate that the

(20) (a) Driess, M.; Hu, H.; Schäufele, H.; Zenneck, U.; Regitz, M.; Rösch, W. *J. Organometal. Chem.* **1987**, *334*, C35. (b) Tolxdorff, C.; Hu, D.; Höferth, B.; Schäufele, H.; Pritzkow, H.; Zenneck, U. *Z. Naturforsch.* **1991**, *46B*, 729.

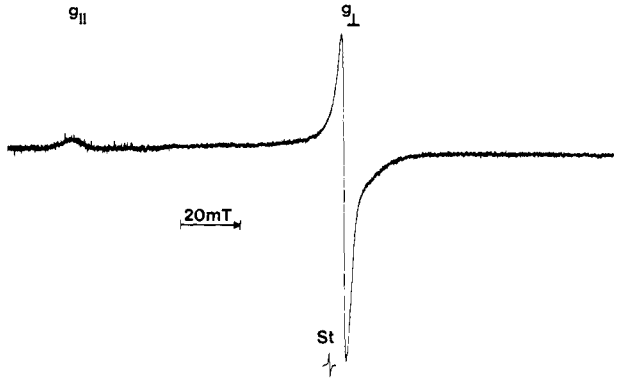

Figure 4. X-band ESR spectrum of **2** at −160 °C in toluene glass (standard, DPPH; g = 2.0036).

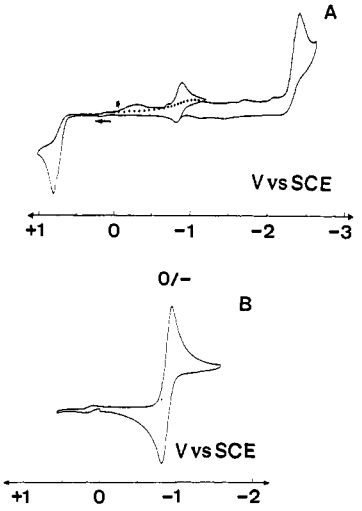

Figure 5. Cyclic voltammograms of **1** (A) and **2** (B) at glassy carbon electrodes vs SCE at 25 °C in 0.1 M Bu_4NPF_6/DME, scan rate 0.1 V s^{-1}.

unpaired electron in **2** and **4** is localized in a metal-centered molecular orbital and are consistent with assignment of a formal oxidation state of Fe(III) in these complexes and, by analogy, in **5**.

Complex **5**, formulated as a bis[iron(III)] complex, is assumed to be a diradical, but unfortunately we were unable to directly observe this property via ESR spectroscopy. Liquid solutions and mixtures in toluene, CH_2Cl_2, dimethylformamide (DMF), or THF in varying concentrations were mostly ESR inactive, as were glasses in these solvents at temperatures down to 50 K. At 35 K, a well-resolved anisotropic spectrum was observed with a rhombic g tensor similar to that of **4** ($g_{\parallel}$ = 2.621 and $g_{\perp}$ = 1.997). No half-field signal ($H_o/2$) was detected. We assume that, owing to the distance of the paramagnetic iron centers from each other (ca. 9.1 Å) and the localization of the unpaired electrons in the vicinity of these centers, weak spin–spin interaction and/or J coupling is responsible for the broadening of the signal to the extent that it is nondetectable in a broad temperature range. Below 50 K, **5** apparently behaves as a diradical with two separate paramagnetic centers, resulting in an ESR spectrum similar to those of **2** and **4**.

Electrochemistry. Cyclic voltammograms of **1**, **2** (Figure 5), and **4**, the data for which are listed in Table IV, underline the redox chemistry of these complexes described earlier. Thus, the air oxidation of **1** to **2**, described above, is paralleled by cyclic voltammetry on **2**, which showed reversible reduction to the monoanion, and also by the simultaneous disappearance of the irreversible signal in the cyclic voltammogram of **1** during bulk electrolysis. A similar effect was produced by bubbling air through the cell as the cyclic voltammograms were recorded. In both cases, the resulting solutions exhibited ESR spectra having g values

Table IV. Cyclic Voltammetry Data[a]

compd	couple	$E°$ [b]	ΔE_p [c]	current ratio[d]	ν [e]	solvent
1	+/0	+0.99	*f*		0.2	DME
	0/−	−2.73	*f*		0.2	DME
2	+/0	+1.07	*f*		0.2	DME
	0/−	−0.88	96	0.98	0.05–20	DME
2	+/0	+1.04	*f*		0.1	MeCN
	0/−	−0.91	70	0.99	0.05–10	MeCN
2	+/0	+1.01	*f*		0.1	CH_2Cl_2
	0/−	−0.96	60	0.99	0.05–2	CH_2Cl_2
3	+/0	+0.84	*f*		0.2	DME
	0/−	−2.29	*f*		0.2	DME
4	+/0	+0.86	*f*		0.2	DME
	0/−	−0.74	90	0.97	0.05–2	DME
	−/2−	−2.32	*f*		0.2	DME
5	+/0	+0.88	*f*		0.2	DME
	0/−	−0.79	130	0.95	0.05–2	DME

[a] Data reported for glassy carbon (GC) working electrodes at room temperature; electrolyte (Bu_4NPF_6) concentration = 0.1 M. [b] Volts vs aqueous SCE; $E°$ reported for reversible systems, peak potentials (E_p^{ox}, E_p^{red} for irreversible systems). [c] Separation in mV of anodic and cathodic peaks; values for reversible systems in DME exceeded 60–70 mV due to uncompensated iR drop. ΔE_p for $Cp_2Fe^{0/+}$ is 100–110 mV under the same conditions. [d] Ratio is given as i_a/i_c for reductions, i_c/i_a for oxidations. [e] Scan rate in V s^{-1}. [f] Irreversible.

identical to **2**. The fact that the reversible wave with E = −0.88 V appears following irreversible reduction of **1** suggests that $\mathbf{2}^-$ forms via hydrogen abstraction from a short-lived $\mathbf{1}^-$ anion; following electrolysis and exposure to air, the observed ESR spectrum was that of **2**.

As was the case in our earlier studies of analogous (η^5-indenyl)ferracarboranes,[1e] these findings support an ECE-type mechanism for both oxidation and reduction. In addition, the stabilizing power of the electron-releasing η^5-C_5Me_5 and η^5-indenyl ligands coordinated to iron is documented by a 250-mV cathodic shift in DME in both cases.[1e,21,22]

Complex **3** was found to undergo irreversible oxidation followed by a reversible signal, but irreversible reduction generated many peaks, indicating the formation of new species, which were unidentified. In contrast, the voltammogram of **4** is readily interpreted as essentially a composite of **1** and **2**. With respect to **5**, the observed reversible wave is interpreted as a 1-electron change, since the paramagnetic iron centers do not communicate, as shown by the ESR observations described above.

Summary

This study further demonstrates the value of the $R_2C_2B_4H_4^{2-}$ ligands both as organometallic synthetic agents and as electronic stabilizers of mono- and dimetallic complexes, allowing the controlled generation and detailed study of a family of species exhibiting varying metal oxidation states. The stability of these complexes under a range of conditions is of central importance; their resistance to degradation permits comprehensive electronic and structural investigation to a degree that is unusual in transition-metal organometallic chemistry, particularly in a nonferrocene system. Extension of the findings on these species to the synthesis and study of larger homologues and similar carborane-based assemblies, including high molecular weight oligomers, is in progress.

Experimental Section

Instrumentation. ^{11}B (115.8- and 64.2-MHz), ^1H (300- and 200-MHz), and ^{13}C (50.3-MHz) FT NMR spectra were acquired on Nicolet NT-360, GE QE300, and Bruker AC-200 spectrometers, and visible–ultraviolet spectra were recorded on a Hewlett-Packard 8452A diode array spectrophotometer with HP Vectra computer interface. Unit-resolution mass spectra were obtained on a Finnegan MAT 4600 GC/MS spectrometer using perfluorotributylamine (FC43) as a calibration standard. Simulated mass spectra based on natural isotopic abundances were calculated on an AT&T 3B5 computer. In all cases, strong parent envelopes were observed, and the calculated and observed unit-resolution

(21) Kölle, U.; Khouzami, F. *Angew. Chem., Int. Ed. Engl.* **1980**, *19*, 640.
(22) El-Murr, N.; Laviron, E. *Can. J. Chem.* **1976**, *54*, 3350.

spectral patterns were in close agreement. High-resolution mass measurements were obtained on a Finnegan MAT 8230 instrument using an SSX 300 data system with perfluorokerosene as a reference standard. Elemental analyses were obtained by the E+R Microanalytical Laboratory, Inc., Corona, NY, and by the Microanalysis Laboratory of the Inorganic Chemistry Institute of the University of Heidelberg. ESR spectra were recorded on Varian E3 and Bruker ESP-300E spectrometers, the latter of which was equipped with a helium cryostat (Oxford Instruments) for low-temperature measurements (100–4.5 K). Infrared spectra were recorded on a Nicolet 5DXB FTIR spectrometer. Column chromatography was conducted on silica gel 60 (Merck), and thick-layer chromatography was carried out on precoated silica gel plates (Merck).

Materials and Procedures. Dichloromethane and *n*-hexane were anhydrous grade and were stored over 4-Å molecular sieves prior to use. THF was distilled from sodium–benzophenone immediately prior to use. *nido*-2,3-Diethyl-2,3-dicarbahexaborane(8) ($Et_2C_2B_4H_6$) was prepared as described elsewhere.[23] Except where otherwise indicated, all syntheses were conducted under vacuum or an atmosphere of nitrogen. Workup of products was generally conducted in air using benchtop procedures.

Electrochemical Studies. Measurements were conducted using a Princeton Applied Research (PAR, EG+G) Model 173 potentiostat, a Model 179 digital coulometer, a Model 175 function generator, a Metrohm electrochemical cell, and Metrohm rotating disk electrodes (Pt, glassy carbon) for polarography and cyclic voltammetry (without rotating). All potentials are given in volts vs an SCE reference electrode which was equipped with a salt bridge (Metrohm) of identical composition with that of the investigated solution. Moderate sweep rate cyclic voltammograms were recorded on a Houston Instrument Series 2000 *x–y* recorder, and rapid scan rate data were obtained on a Tektronix 2224 two-channel 60-MHz storage oscilloscope connected to a microcomputer.

Purification of electrolytes and solvents and all measurements were conducted under argon. Bu_4NPF_6 (Fluka electrochemical reagent grade) was dried at 110 °C for 20 h in vacuo before use. Dichloromethane (Merck p.a.; Riedel-deHaen 99+%) was distilled from CaH_2 and stored under argon in the dark. DME (Aldrich 99+%) was passed through a column of activated basic alumina (ICN Alumina B Super I, activated at 280 °C for 2 days under vacuum) and distilled twice before use. Solvents were stored under argon, and freshly prepared solutions of electrolytes were stored in Schlenck tubes equipped with Teflon valves. Solutions (0.1 M) of electrolytes were prepared by fractional distillation of all solvents directly into the Schlenck tube containing the salt, thus providing 100-mL samples of highly purified solutions in one step.

Preparation of $Cp^*Fe^{II}H(Et_2C_2B_4H_4)$ (1). Using a procedure analogous to that described earlier[12] for the synthesis of $Cp^*Co(Et_2C_2B_4H_4)$, 0.955 g (7.50 mmol) of $FeCl_2$ and an equimolar quantity of $Li^+C_5Me_5^-$ were combined in THF solution, forming an olive-green solution of Cp^*FeCl_x. This solution was frozen in liquid nitrogen and a solution of 7.5 mmol of $Na^+Et_2C_2B_4H_5^-$ in THF was added in vacuo through a frit. The mixture was thawed and stirred overnight at room temperature, forming an orange-brown solution which was opened to the air. The solvent was removed by rotary evaporation, and the residue was taken up in hexane and passed through 3 cm of silica gel, affording a single orange band which on evaporation of solvent gave crystalline **1**, isolated yield 1.96 g (6.08 mmol, 82%). Exact Mass Calcd for $^{56}Fe^{12}C_{16}{}^{11}B_4{}^1H_{30}{}^+$: 322.2069. Found: 322.2076. Anal. Calcd for $FeC_{16}B_4H_{30}$: C, 59.77; H, 9.41. Found: C, 59.90; H, 9.48. Vis–UV (nm, in CH_2Cl_2): 460 (11%), 294 (100%), 248 (93%). Ir (neat film, cm^{-1}): B–H, 2557; C–H, 2873, 2914, 2932, 2968.

Preparation of $Cp^*Fe^{III}(Et_2C_2B_4H_4)$ (2). A 0.713-g (2.2 mmol) sample of **1** was dissolved in 10 mL of wet TMEDA, producing an immediate color change from orange to dark gray (nearly black). After 1 h of stirring, the TMEDA was removed and the residue was taken up in hexane and placed on a 5-cm silica column and washed with hexane followed by dichloromethane. A single dark gray band was obtained, from which 0.640 g (1.99 mmol, 90%) of nearly black crystals of **2** was collected. Exact Mass Calcd for $^{56}Fe^{12}C_{16}{}^{11}B_4{}^1H_{29}{}^+$: 321.1991. Found: 322.1994. Anal. Calcd for $FeC_{16}B_4H_{29}$: C, 59.96; H, 9.12. Found: C, 60.14; H, 9.26. Visible–UV (nm, in CH_2Cl_2): 586 (2%), 474 (5%), 302 (89%), 274 (100%), 234 (49%). IR (neat film, cm^{-1}): B–H, 2534; C–H, 2965, 2972.

^1H and ^{13}C NMR Spectroscopy on 2 and 2^-. The method of Zenneck et al.[10] was employed on a nearly saturated solution of **2** in THF-d_8 in a NMR tube which had been prepared with a potassium mirror in its central section. The solution was introduced into the bottom of the tube via a capillary delivery tube so that no contact was made with the potassium, and the tube was sealed under vacuum. Proton and carbon NMR spectra at 200 and 50.3 MHz, respectively, were recorded for pure paramagnetic **2**, and the tube was then tilted to permit brief contact of the solution with the potassium, producing partial reduction to 2^-, after which NMR spectra were again recorded. In obtaining the ^{13}C spectra, decoupling frequencies taken from the proton NMR observations were used to decouple the quartets. Repetition of this procedure produced incremental conversion to the diamagnetic anion 2^-, ultimately forming a pure solution of the latter whose NMR spectra showed no further change on contact with the potassium.

Preparation of $[(Et_2C_2B_4H_4)FeH(C_5Me_4)]_2C_6H_4$ (3). The procedure employed earlier[5] for the synthesis of $[(Et_2C_2B_4H_4)Co(C_5Me_4)]_2C_6H_4$ was used. A solution of the $(C_5Me_4)_2C_6H_4{}^{2-}$ dianion was prepared by deprotonation of 0.97 g (6.10 mmol) of the neutral hydrocarbon[14] with butyllithium in THF; this solution was added slowly to an equivalent amount of ferrous chloride suspended in THF. After stirring this dark orange-brown solution for 45 min, 6.1 mmol of $Na^+Et_2C_2B_4H_5^-$ in THF was filtered onto the iron complex, producing an instant color change to tomato red with no gas evolution. The solution was stirred for 2 h at room temperature and then opened to the air and the solvent removed by rotary evaporation, affording a brown solid which was taken up in dichloromethane and filtered through silica. The orange solution was evaporated to dryness and the residue taken up in 50/50 CH_2Cl_2/hexane and chromatographed on silica, giving one orange band which was collected and characterized as orange crystalline **3**, 1.275 g (1.85 mmol, 60.2%). Anal. Calcd for $Fe_2C_{36}B_8H_{58}$: Fe, 16.21; C, 62.75; B, 12.55; H, 8.48. Found: Fe, 16.13; C, 62.78; B, 12.48; H, 8.41. Visible–UV (nm, in CH_2Cl_2): 272 (100%), 246 (88%).

Deprotonation of 3 and Reprotonation of 3^{2-}. In a typical experiment, 65 mg (0.113 mmol) of **3** in 10 mL of THF was treated with 0.09 mL of 2.5 M *n*-butyllithium in hexanes, giving immediately a crimson solution of the postulated 3^{2-} ion. Addition of 10 mL of 1.5 mL of aqueous HCl to this solution regenerated orange solution of **3**, which on workup (evaporation to dryness and extraction with CH_2Cl_2 followed by chromatography on silica) afforded orange **3** in 98% yield. When THF solutions of 3^{2-} were opened to air and stirred overnight, conversion to **3** was again quantitative.

Formation of $(Et_2C_2B_4H_4)Fe^{II}H(C_5Me_4)$–$C_6H_4$–$(C_5Me_4)Fe^{III}(Et_2C_2B_4H_4)$ (4) and $[(Et_2C_2B_4H_4)Fe^{III}(C_5Me_4)]_2C_6H_4$ (5). **(a) Via TMEDA in Air.** A 150-mg sample (0.22 mmol) of **3** was dissolved in 10 mL of TMEDA, and 3 drops of water were added. Within 30 min the solution had turned dark brown. The volatiles were removed by evaporation, and the residue was dissolved in CH_2Cl_2 and chromatographed on silica, giving a major band of black crystalline **5** (128 mg, 85.6%) and a minor band of black crystalline **4** (12 mg, 8.5%).

(b) Via Ethyl Acetate. A 100-mg sample of **3** (0.145 mmol) was dissolved in 10 mL of acidified ethyl acetate (prepared by combining 50 mL of ethyl acetate with 10 mL of concentrated HCl and removing the aqueous phase) and 10 mL of THF, giving a dark green solution. After 1 h the solvent was removed by rotary evaporation, affording a quantitative yield of black **5**.

Conversion of 5 to 4. A solution of 100 mg of **5** (0.15 mmol) in 50 mL of THF was added in vacuo to a flask in which a potassium mirror had been prepared, and the reaction mixture was stirred for 1 h at room temperature. The solution was opened to the air and the solvent was removed by evaporation. The residue was dissolved in 20:80 CH_2Cl_2/hexane and eluted on a silica gel column in the same solvent. Four bands were obtained, consisting of red **3** (40 mg, 50% based on starting material consumed), dark green $(Et_2C_2B_4H_4)Fe^{II}H(C_5Me_4)$–$C_6H_4$–$(C_5Me_4H)$ (10%, a decomposition product identified from its mass spectrum), greenish-brown **4** (30 mg, 38%), and unreacted dark green **5** (20 mg).

X-ray Structure Determination on 3. A unique set of intensities (*hkl* range ±12,+21,+20) was collected on a Siemens-Stoe 4-circle diffractometer, using the ω-scan technique, with data collection parameters as given in Table II. Reflections for which $I > 2\sigma(I)$ were considered observed, and only these reflections were employed in the final refinement of structural parameters. An empirical absorption correction (parameters in Table II) was applied. The structure was solved by the heavy atom method and refined by least-squares calculations employing anisotropic thermal parameters for all non-hydrogen atoms. All hydrogen atoms were located in a difference Fourier map and refined isotropically, the refinement converging to the R and R_w values given in Table II. Scattering factors were taken from Cromer and Mann.[24] All calculations were carried out using the programs SHELX76 and SHELXS86.[25]

Acknowledgment. This work was supported by NATO International Collaborative Research Grant 0196/85, by the Deutsche Forschungsgemeinschaft SFB 247, by the U.S. Army Research

(23) Boyter, H. A., Jr.; Swisher, R. G.; Sinn, E.; Grimes, R. N. *Inorg. Chem.* **1985**, *24*, 3810.

(24) Cromer, D. T.; Mann, J. B. *Acta Crystallogr.* **1968**, *A24*, 321.

(25) Sheldrick, G. M. SHELX76 program for crystal structure determination, Cambridge, 1976; SHELXS86, Göttingen, 1986.

Office (R.N.G.), and by National Science Foundation Grant CHE 8721657 (to R.N.G.). We thank Thomas Sutto (University of Virginia) for the magnetic susceptibility measurements and Dr. P. Such (Bruker GMBH, Rheinstetten, Germany) for recording ESR spectra at liquid helium temperature.

Supplementary Material Available: Tables of atom coordinates, anisotropic thermal parameters, and mean planes for **3** and of ^1H and ^{13}C NMR data for $2/2^-$ mixtures (5 pages); tables of calculated and observed structure factors (9 pages). Ordering information is given on any current masthead page.

Semiconductor Nanocrystals Covalently Bound to Metal Surfaces with Self-Assembled Monolayers

V. L. Colvin, A. N. Goldstein, and A. P. Alivisatos*

Contribution from the Department of Chemistry, University of California, Berkeley, and Materials Sciences Division, Lawrence Berkeley Laboratory, Berkeley, California 94720.
Received March 11, 1991. Revised Manuscript Received March 2, 1992

Abstract: A method is described for attaching semiconductor nanocrystals to metal surfaces using self-assembled difunctional organic monolayers as bridge compounds. Three different techniques are presented. Two rely on the formation of self-assembled monolayers on gold and aluminum in which the exposed tail groups are thiols. When exposed to heptane solutions of cadmium-rich nanocrystals, these free thiols bind the cadmium and anchor it to the surface. The third technique attaches nanocrystals already coated with carboxylic acids to freshly cleaned aluminum. The nanocrystals, before deposition on the metals, were characterized by ultraviolet-visible spectroscopy, X-ray powder diffraction, resonance Raman scattering, transmission electron microscopy (TEM), and electron diffraction. Afterward, the nanocrystal films were characterized by resonance Raman scattering, Rutherford back scattering (RBS), contact angle measurements, and TEM. All techniques indicate the presence of quantum confined clusters on the metal surfaces with a coverage of approximately 0.5 monolayers. These samples represent the first step toward synthesis of an organized assembly of clusters as well as allow the first application of electron spectroscopies to be completed on this type of cluster. As an example of this, the first X-ray photoelectron spectra of semiconductor nanocrystals are presented.

Introduction

The ability to assemble molecules into well-defined two- and three-dimensional spatial configurations is a major goal in the field of self-assembled monolayers (SAMs).[1] Since the discovery that alkanethiols will displace practically any impurity on a gold surface[2] and will spontaneously create an ordered monolayer of high quality,[3] interest in these systems has been extensive.[4-6] Recent advances have extended SAMs beyond the prototype gold/thiol systems. Fatty acids on aluminum,[7] silanes on silicon,[8] isonitriles on platinum,[9] and rigid phosphates on metals[10] are examples. In addition to the wide choice of the substrate, the chemical functionality presented at the top of a monolayer can be controlled by replacing monofunctional alkanes with difunctional organic compounds.[11] Such assemblies can then be used to build up more complex structures in three dimensions,[12] enabling chemists to engineer complex organic structures on top of macroscopic surfaces. This specific control over the microscopic details of interfaces has allowed for diverse applications of SAMs. Metals, for example, provide the ideal support for organic compounds with large nonlinear optical behavior, and by using SAMs the molecules can be held in specific orientations with respect to the metal.[13] In other work, the ability to dictate the structural details of an interface is exploited to study processes of electron transport between an electrode surface and an active moiety bound on top of a monolayer.[14] We employ the well-developed chemistry of SAMs to attach an interesting compound, a semiconductor nanocrystal, to metal surfaces. The incorporation of clusters into the monolayers is a first step toward creating arrays of quantum dots, and the total assembly of clusters on metals represents a new kind of material with many potential uses. This new sample geometry allows us to apply photoelectron spectroscopy to semiconductor nanocrystals for the first time.

Semiconductor nanocrystals have been the subject of numerous spectroscopic investigations in recent years;[15-19] the origin of the extensive interest is that the absorption spectrum of the clusters is a strong function of their radii.[20] The clusters, in this work, cadmium sulfide, range in size from 10 to 100 Å in radius, and as their radius decreases, the electronic wave functions are confined, causing the absorption edge to shift to the blue by as much as 1 V.[20b] Despite these dramatic changes in electronic structure, only optical spectroscopies have been used to study these systems.

(1) Whitesides, G. M. *Chimia* **1990**, *44*, 310-311.
(2) Nuzzo, R. G.; Allara, D. L. *J. Am. Chem. Soc.* **1983**, *105*, 4481-4483.
(3) Porter, M. D.; Bright, T. B.; Allara, D. L.; Chidsey, C. E. D. *J. Am. Chem. Soc.* **1987**, *109*, 3559-3568.
(4) Tillman, N.; Ulman, A.; Elman, J. F. *Langmuir* **1989**, *5*, 1020-1026.
(5) Reubinstein, I.; Steinberg, S.; Tor, Y.; Shanzer, A.; Sagiv, J. *Nature* **1988**, *332*, 426-429.
(6) Bravo, B. G.; Michelhaugh, S. L.; Soriaga, M. P. *Langmuir* **1989**, *5*, 1092-1095.
(7) Allara, D. L.; Nuzzo, R. G. *Langmuir* **1985**, *1*, 45-52.
(8) (a) Maoz, R.; Sagiv, J. *Langmuir* **1987**, *3*, 1045-1051. (b) Maoz, R.; Sagiv, J. *Langmuir* **1987**, *3*, 1034-1044. (c) Wasserman, S. R.; Tao, Y.; Whitesides, G. M. *Langmuir* **1989**, *5*, 1074-1087.
(9) Hickman, J. J.; Zou, C.; Ofer, D.; Harvey, P. D.; Wrighton, M. S.; Laibinis, P. E.; Bain, C. D.; Whitesides, G. M. *J. Am. Chem. Soc.* **1989**, *111*, 7271-7272.
(10) Lee, H.; Kepley, L. J.; Hong, H.; Akhter, S.; Mallouk, T. E. *J. Phys. Chem.* **1988**, *92*, 2597-2601.
(11) (a) Bain, C. D.; Evall, J.; Whitesides, G. M. *J. Am. Chem. Soc.* **1989**, *111*, 7155-7164. (b) Pale-Grosdemange, C.; Simon, E. S.; Prime, K. L.; Whitesides, G. M. *J. Am. Chem. Soc.* **1991**, *113*, 12-20.
(12) (a) Ulman, A.; Tillman, N. *Langmuir* **1989**, *5*, 1418-1420. (b) Tillman, N.; Ulman, A.; Reuner, T. L. *Langmuir* **1989**, *5*, 101-105.
(13) Putvinski, T. M.; Schilling, M. L.; Katz, H. E.; Chidsey, C. E. D.; Mujsce, A. M.; Emerson, A. B. *Langmuir* **1990**, *6*, 1567-1571.
(14) (a) Chidsey, C. E. D. *Science* **1991**, *251*, 919-922. (b) Chidsey, C. E. D.; Bertozzi, C. R.; Putvinski, T. M.; Mujsce, A. M. *J. Am. Chem. Soc.* **1990**, *112*, 4301-4306. (c) Chidsey, C. E. D.; Loiacono, D. N. *Langmuir* **1990**, *6*, 682-691.
(15) Alivisatos, A. P.; Harris, A. L.; Levinos, N. J.; Steigerwald, M. L.; Brus, L. E. *J. Chem. Phys.* **1988**, *89*, 4001-4011.
(16) (a) Spanhel, L.; Hasse, M.; Weller, H.; Henglein, A. *J. Am. Chem. Soc.* **1987**, *109*, 5649-5655. (b) Hasse, M.; Weller, H.; Henglein, A. *J. Phys. Chem.* **1988**, *92*, 482-487. (c) Fischer, C. H.; Henglein, A. *J. Phys. Chem.* **1989**, *93*, 5578.
(17) Nosaka, Y.; Yamaguchi, K.; Miyama, H.; Hayashi, A. *Chem. Lett.* **1988**, 605.
(18) Hayes, D.; Micic, I. O.; Nenadovic, M. T.; Swayambunathan, V.; Meisel, D. *J. Phys. Chem.* **1989**, *93*, 4603.
(19) Herron, N.; Wang, Y.; Eckert, H. *J. Am. Chem. Soc.* **1990**, *112*, 1322.
(20) (a) Brus, L. E. *J. Chem. Phys.* **1984**, *80*, 4403-4409. (b) Brus, L. E. *J. Chem. Phys.* **1986**, *90*, 2555-2560.

0002-7863/92/1514-5221$03.00/0